Net-baryon number fluctuations in the quark-meson-nucleon model at finite density

Michał Marczenko, Chihiro Sasaki

Institute of Theoretical Physics
University of Wrocław, Poland

arXiv:1711.05521 [hep-ph]

EMMI Workshop
GSI, 12.02.2018

Uniwersytet Wrocławski

National Science Centre Poland

Outline

Parity doubling in $N_f = 2 + 1$ LQCD Aarts *et al*, JHEP **1706**, 034 (2017)

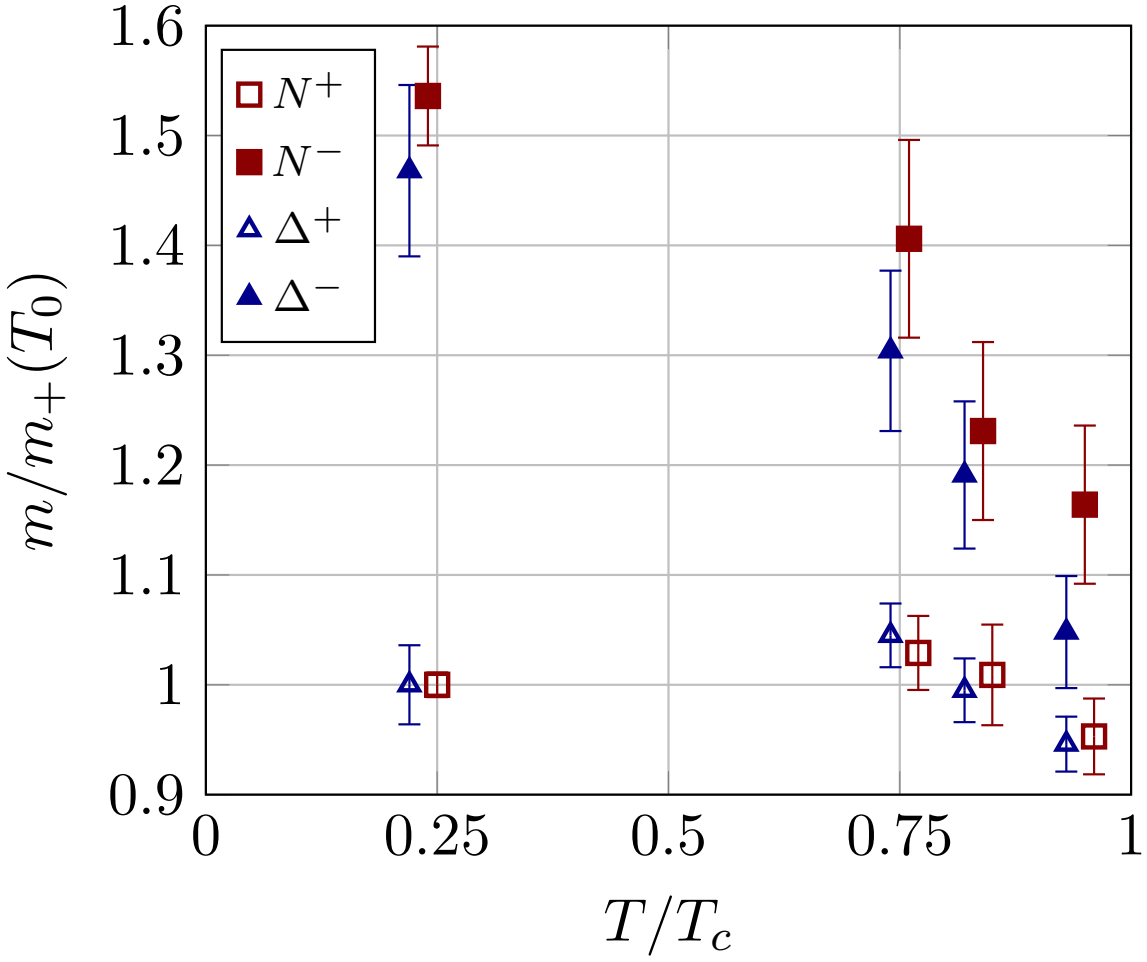

Despite unphysical $m_\pi \approx 384$ MeV and $T_c \approx 185$ MeV:

- Imprint of chiral symmetry restoration
- Signature of parity-doublet structure

Realization in chiral models DeTar, Kunihiro Phys. Rev. D **39** 2805 (1989)

- Naive and mirror assignments under $SU(2)_L \times SU(2)_R$

$$\mathcal{L}_N = i\bar{\psi}_1 \partial\!\!\!/ \psi_1 + i\bar{\psi}_2 \partial\!\!\!/ \psi_2 + m_0 \left(\bar{\psi}_1 \gamma_5 \psi_2 - \bar{\psi}_2 \gamma_5 \psi_1 \right)$$

  For finite m_0, chiral symmetry is
  - explicitly broken under naive assignment
  - remains unbroken under mirror assignment
- Parity doublet model for cold and dense nuclear matter

  Zschiesche *et al*, Phys. Rev. C **75**, 055202 (2007)

$$\mathcal{L} = \mathcal{L}_N + \sum_{k=1,2} g_k \bar{\psi}_k \left(\sigma \pm i\gamma_5 \boldsymbol{\tau} \cdot \boldsymbol{\pi} \right) \psi_k - g_\omega \bar{\psi}_k \omega\!\!\!/ \psi_k + \mathcal{L}_M$$

  - Fermions coupled to bosons: σ, π, ω
  - $\mathcal{L}_M \rightarrow$ Linear σ-model

Parity-doublet mass structure: $(\psi_1, \psi_2) \to (N_+, N_-)$

$$m_\pm = \frac{1}{2}\left[\sqrt{(g_1+g_2)\,\sigma + 4m_0^2} \mp (g_1-g_2)\,\sigma\right] \xrightarrow{\sigma\to 0} m_0$$

- particle identification: $N_+ \to N(939)$, $N_- \to N(1535)$
- high $m_0 \sim 790$ MeV favored by incompressibility and LQCD

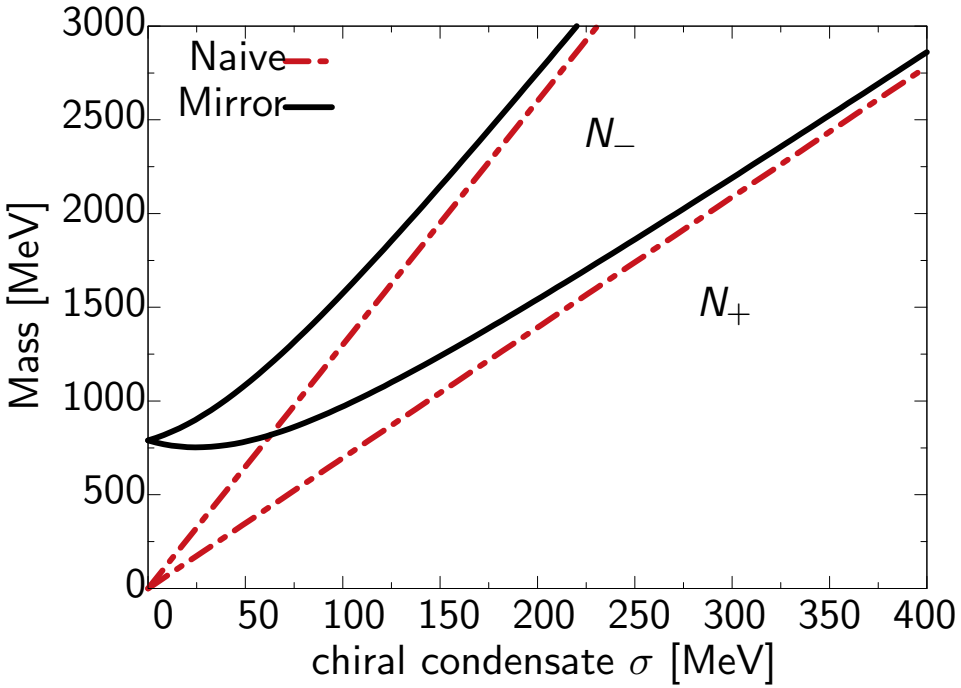

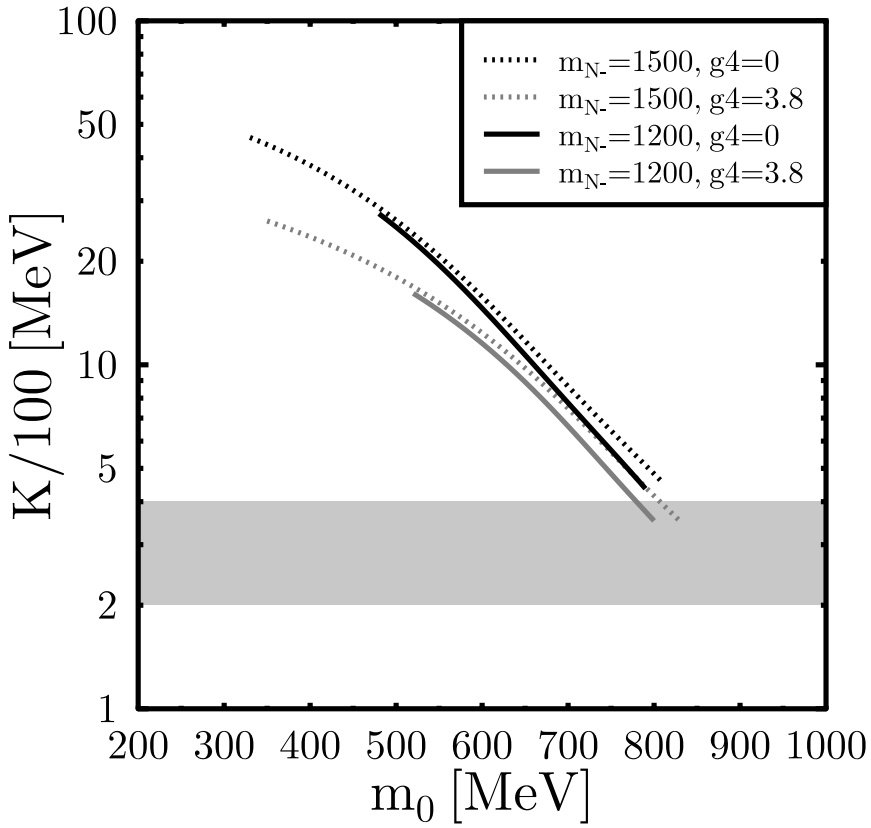

Zschiesche *et al*, Phys. Rev. C **75**, 055202 (2007)

Hybrid quark-meson-nucleon model Benić *et al*, Phys. Rev. D **91**, 125034 (2015)

Parity doublet model + quark-meson coupling

$$\mathcal{L}_q = \bar{q} i \partial\!\!\!/ q + g_q \bar{q} \left(\sigma + i\gamma_5 \boldsymbol{\tau} \cdot \boldsymbol{\pi}\right) q - V_\sigma$$

Statistical confinement:

- IR cutoff for quarks: $f_q \to \theta\left(\boldsymbol{p}^2 - b^2\right) f_q$
- UV cutoff for nucleons: $f_\pm \to \theta\left(\alpha^2 b^2 - \boldsymbol{p}^2\right) f_\pm$
- α - new model parameter (to be studied here)

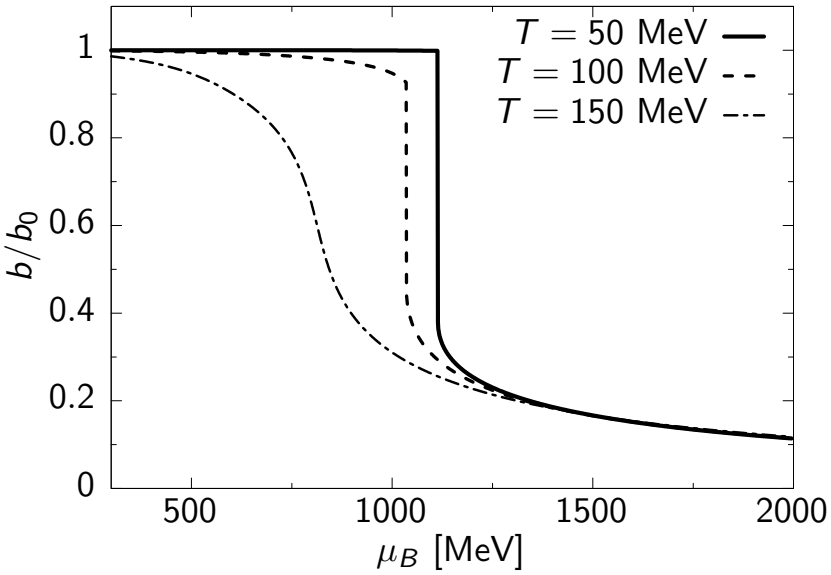

- b - scalar field

$$V_b = -\frac{1}{2}\kappa_b^2 b^2 + \frac{1}{4}\lambda_b b^4$$

$b(\mu_B = 0) > 0$ favors nucleons

$b(\mu_B \to \infty) = 0$ favors quarks

Results at $T = 10$ MeV ($\alpha b_0 = 390$ MeV)

- Mean field approximation $\rightarrow$ gap equations

$$\frac{\partial \Omega}{\partial \sigma} = \frac{\partial \Omega}{\partial \omega} = \frac{\partial \Omega}{\partial b} = 0$$

- Fixed to the nuclear groundstate properties at $T = 0$:
  - Binding energy: $E/A - m_+ = -16$ MeV
  - Saturation density: $\rho_0 = 0.16$ fm^{-3}

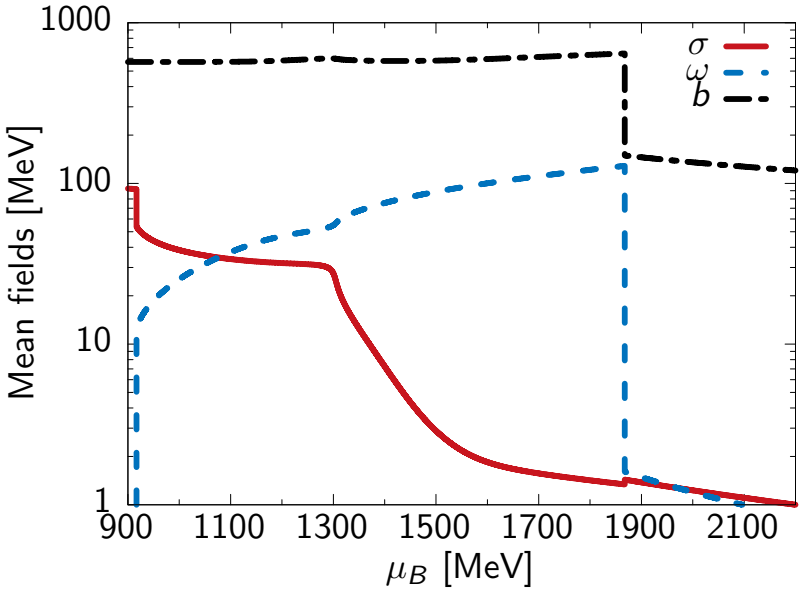

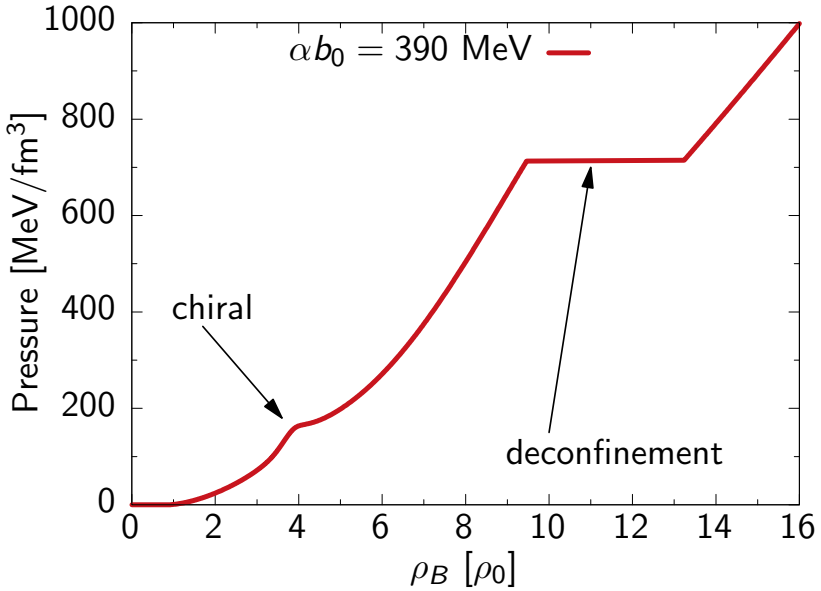

Matter composition at $T = 10$ MeV ($\alpha b_0 = 390$ MeV)

$$Y_x = \frac{\rho_x}{\rho_+ + \rho_- + \rho_q}$$

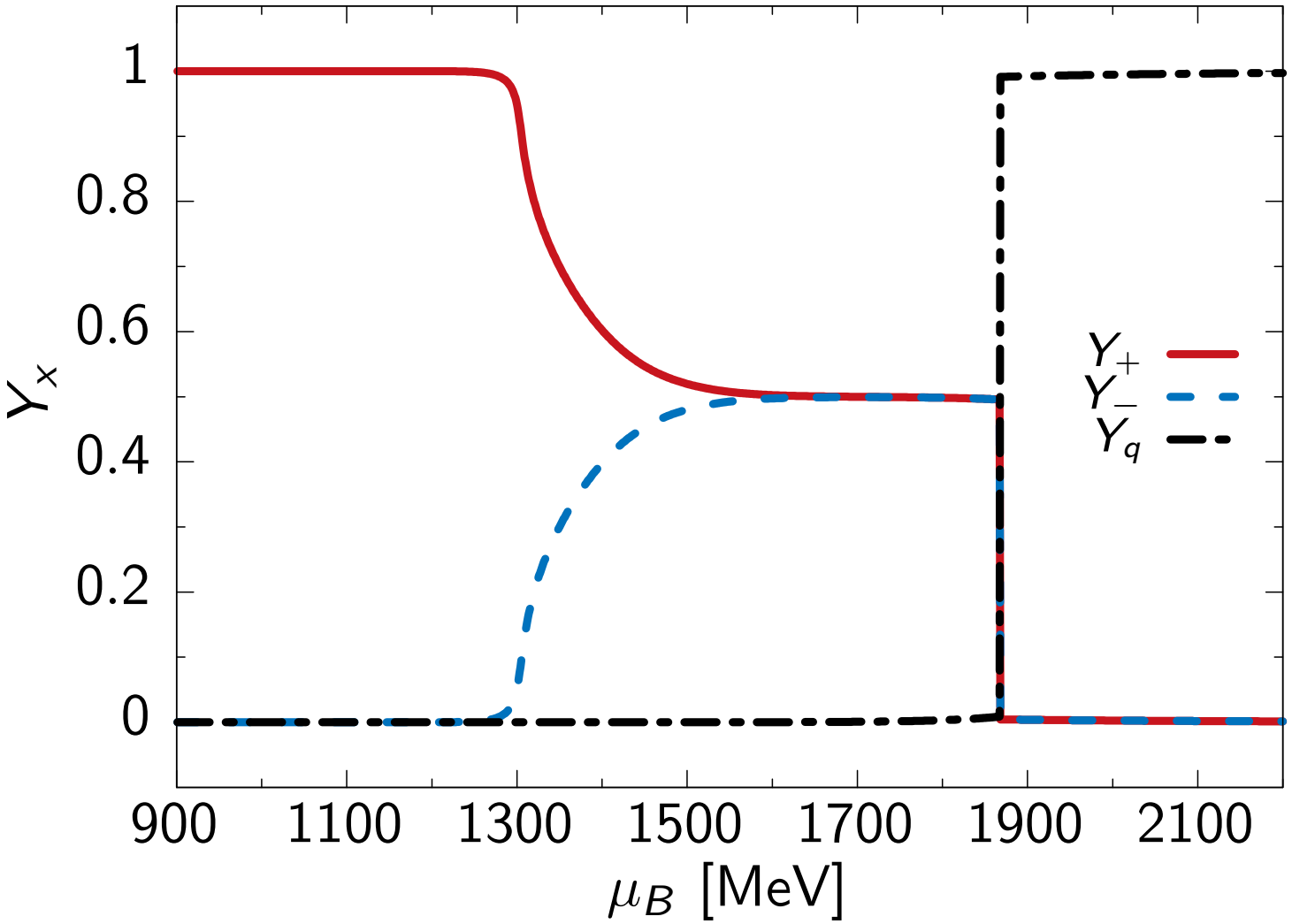

Model phase diagram at $T = 10$ MeV

- Deconfinement always of 1st order (by the choice of V_b)
- Order of chiral transition (from low to high α)

$$\text{1st order} \rightarrow \text{Critical Point} \rightarrow \text{crossover}$$

- Sequential phase transitions (may coincide for smaller m_0)

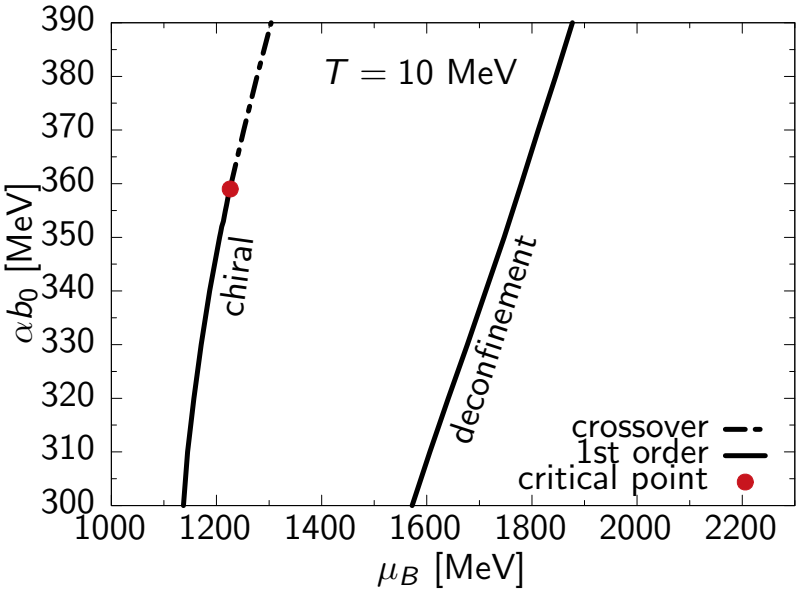

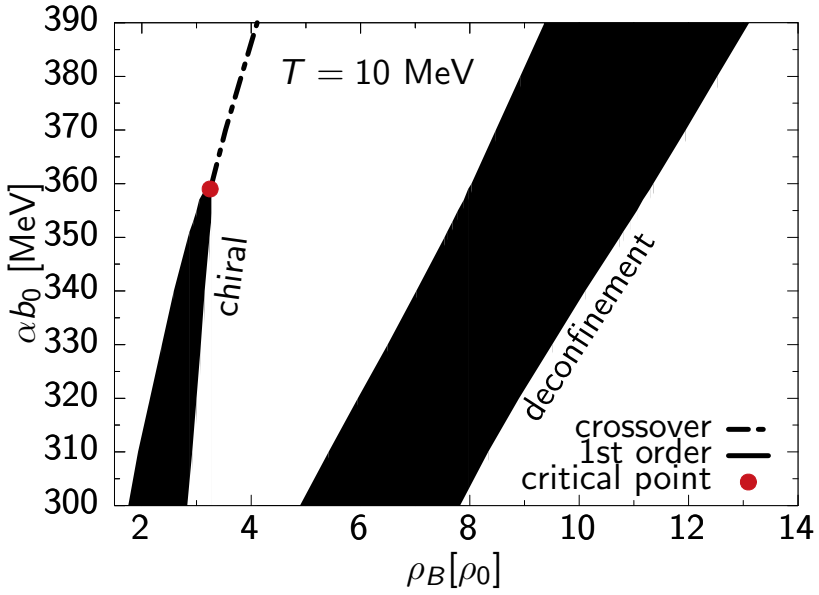

Model phase diagram at higher temperatures

- Thermal excitations $\rightarrow$ quarks appear before deconfinement
- Quark density $< 1\%$ of total density at deconfinement

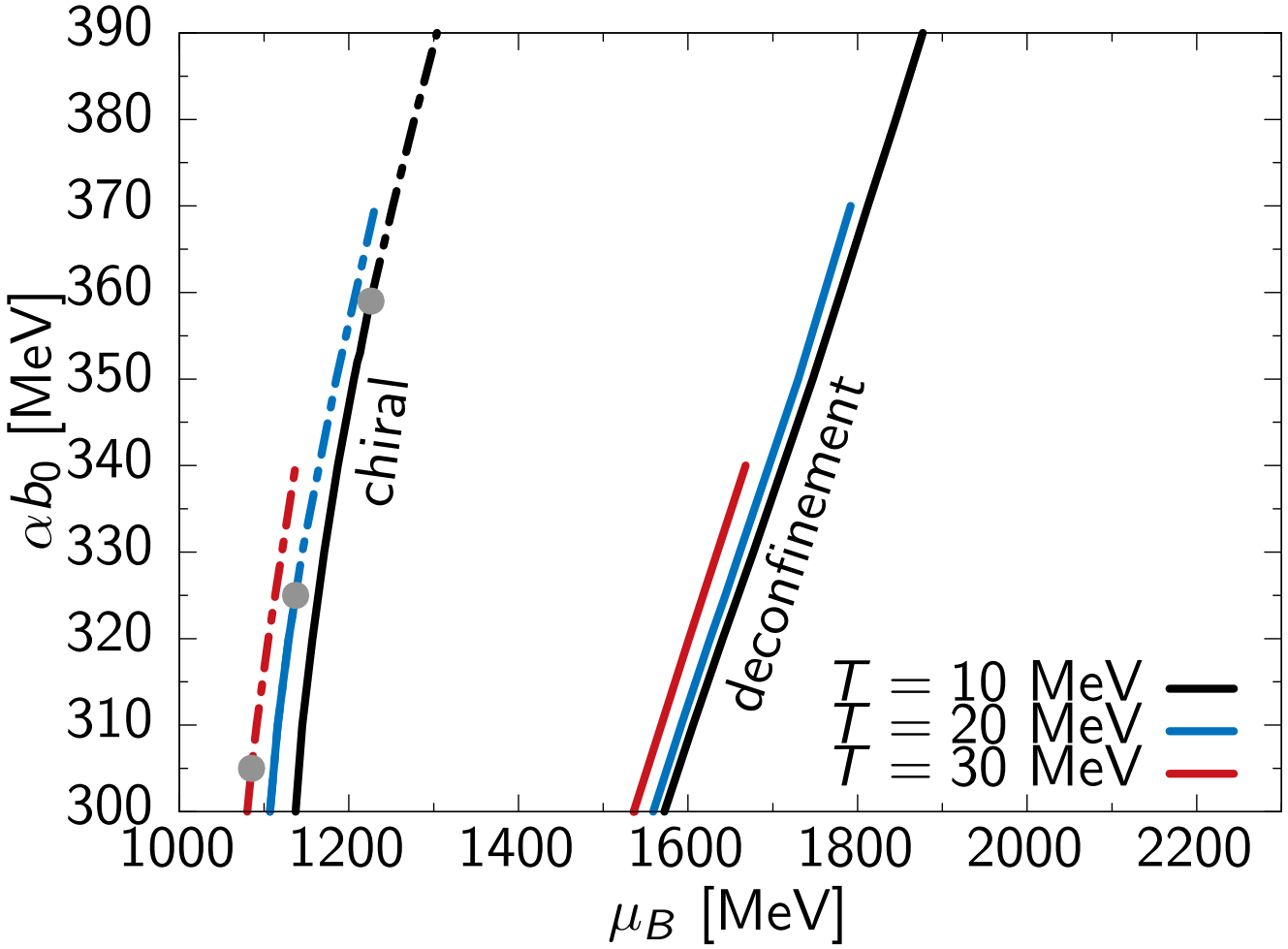

Higher-order cumulants: χ_2 at $T = 10$ MeV

- NJL: no confinement mechanism
- Parity doublet: wrong asymptotics

HQMN resembles all these features

- Confinement mechanism **strengthens** chiral transition
- Higher-order cumulants **less sensitive** to deconfinement

Generalized susceptibilities

$$\chi_n = -\frac{1}{\mu_B^{n-4}} \frac{\partial^n \Omega}{\partial \mu_B^n}$$

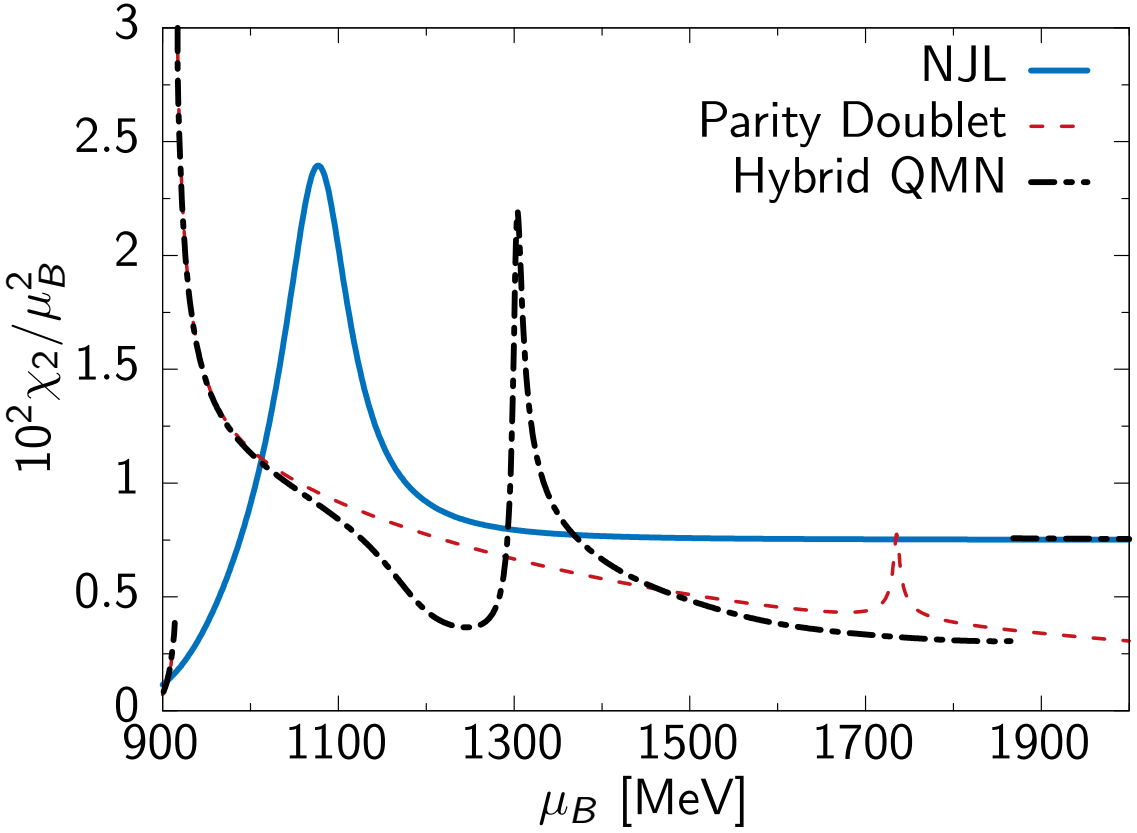

Higher-order cumulants: χ_3 at $T = 10$ MeV

- NJL: no confinement mechanism
- Parity doublet: wrong asymptotics

HQMN resembles all these features

- Confinement mechanism **strengthens** chiral transition
- Higher-order cumulants **less sensitive** to deconfinement

Generalized susceptibilities

$$\chi_n = -\frac{1}{\mu_B^{n-4}} \frac{\partial^n \Omega}{\partial \mu_B^n}$$

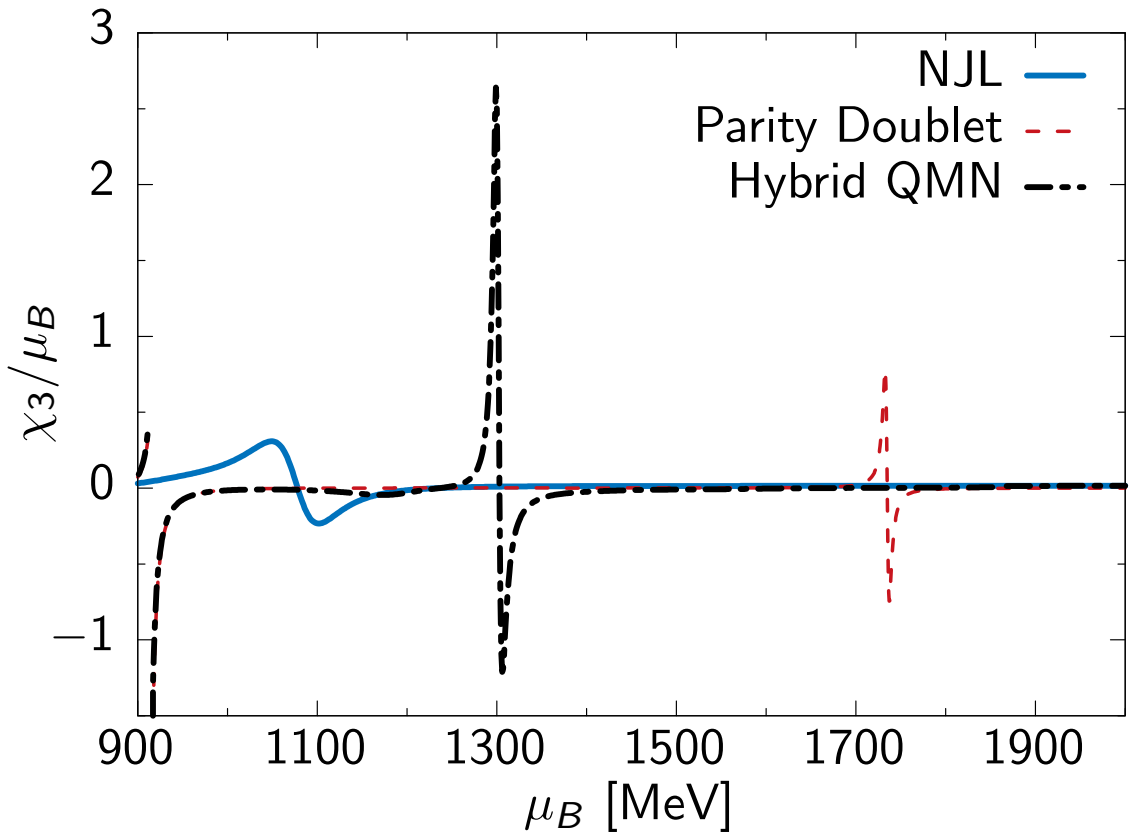

Higher-order cumulants: χ_4 at $T = 10$ MeV

- NJL: no confinement mechanism
- Parity doublet: wrong asymptotics

HQMN resembles all these features

- Confinement mechanism **strengthens** chiral transition
- Higher-order cumulants **less sensitive** to deconfinement

Generalized susceptibilities

$$\chi_n = -\frac{1}{\mu_B^{n-4}} \frac{\partial^n \Omega}{\partial \mu_B^n}$$

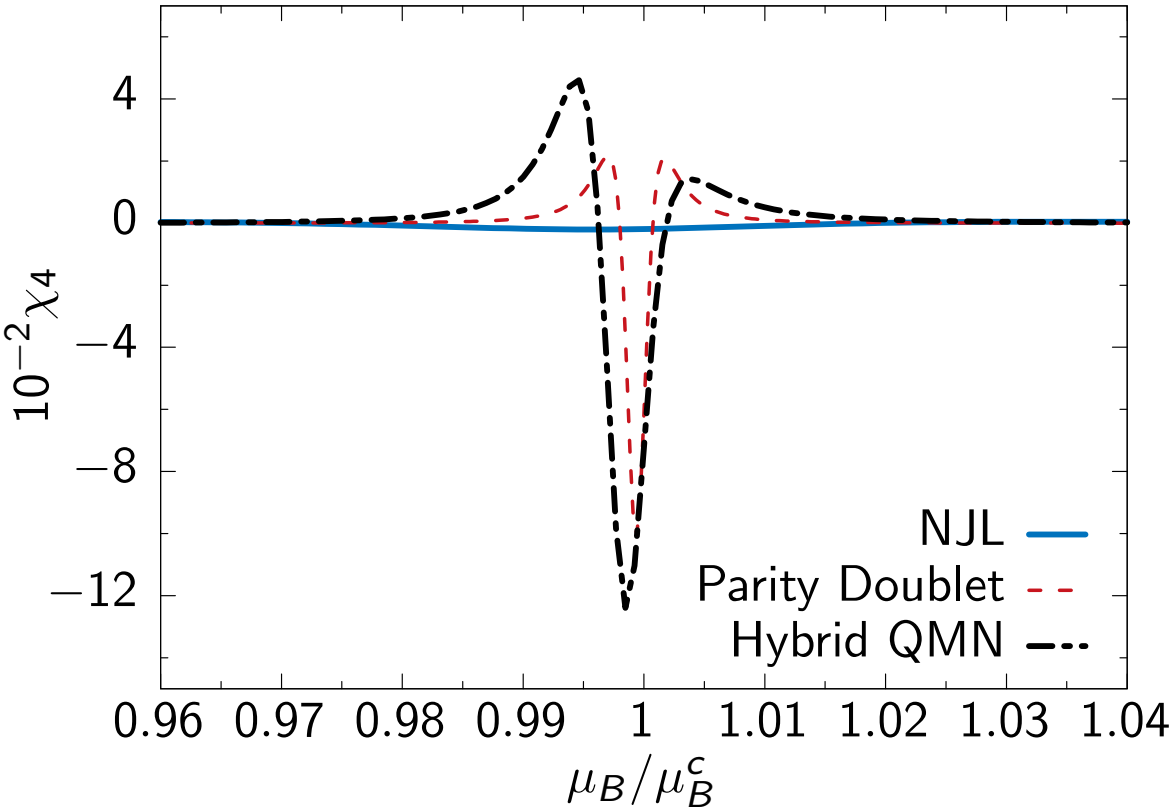

Conclusions

Hybrid QMN model offers a unified approach to cold and dense QCD matter:

- Influence of statistical confinement on chiral transition:
  - triggered at **much earlier** baryon chemical potential
  - **strengthened** in comparison to the hadronic-model result
- Higher-order cumulants rather **insensitive** to deconfinement:
  - Influence of different potentials $\longrightarrow$ crossover transition
  - connection to a symmetry of QCD

    QCD-like theory $\longrightarrow$ A. Cherman *et al*, Phys. Rev. Lett. **119** (2017) no.22, 222001

Thank you for your attention

Full HQMN model Lagrangian

- $\mathcal{L} = \mathcal{L}_N + \mathcal{L}_M + \mathcal{L}_q$

$$
\begin{aligned}
\mathcal{L}_N &= \sum_{k=1,2} \bar{\psi}_k i\partial\!\!\!/ \psi_k + m_0 \left(\bar{\psi}_2 \gamma_5 \psi_1 - \bar{\psi}_1 \gamma_5 \psi_2\right) \\
&\quad + \sum_{k=1,2} g_k \bar{\psi}_k \left(\sigma \pm i\gamma_5 \boldsymbol{\tau} \cdot \boldsymbol{\pi}\right) \psi_k - g_\omega \bar{\psi}_k \omega\!\!\!/ \psi_k \\
\mathcal{L}_q &= \bar{q} i\partial\!\!\!/ q + g_q \bar{q} \left(\sigma + i\gamma_5 \boldsymbol{\tau} \cdot \boldsymbol{\pi}\right) q \\
\mathcal{L}_M &= \frac{1}{2}(\partial_\mu \sigma)^2 + \frac{1}{2}(\partial_\mu \boldsymbol{\pi})^2 - \frac{1}{4} F_{\mu\nu} F^{\mu\nu} - V_\sigma - V_\omega - V_b \\
V_\sigma &= -\frac{1}{2}\bar{\mu}^2 \left(\sigma^2 + \boldsymbol{\pi}^2\right) + \frac{\lambda}{4}(\sigma^2 + \boldsymbol{\pi}^2)^2 - \epsilon\sigma \\
V_\omega &= -\frac{1}{2} m_\omega^2 \omega_\mu \omega^\mu \\
V_b &= -\frac{1}{2}\kappa_b^2 b^2 + \frac{1}{4}\lambda_b b^4
\end{aligned}
$$

Higher-order cumulants: χ_4/χ_2 at $T = 10$ MeV

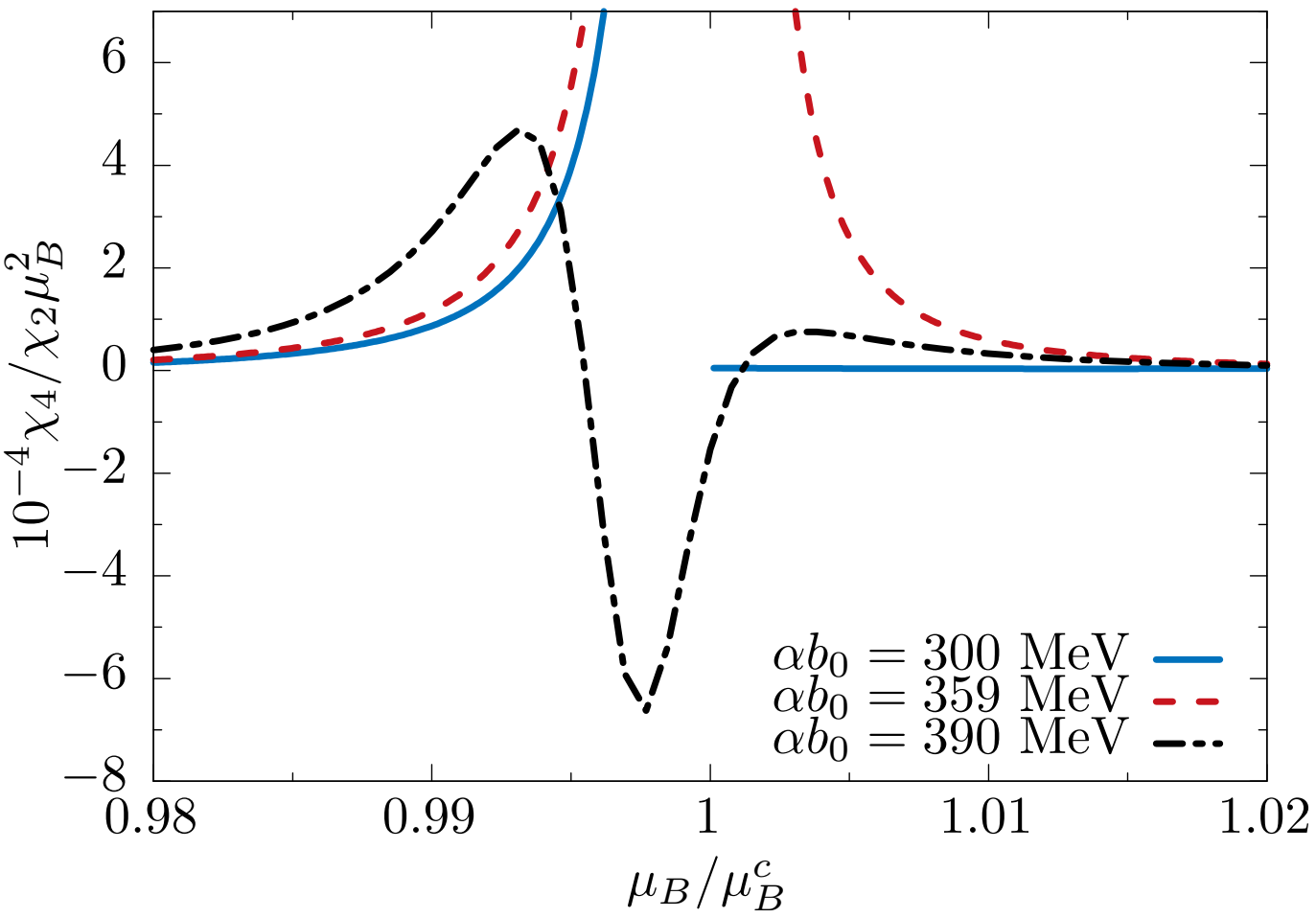

Phase diagram in $(T - \mu_B)$-plane ($\alpha b_0 = 310$ MeV)

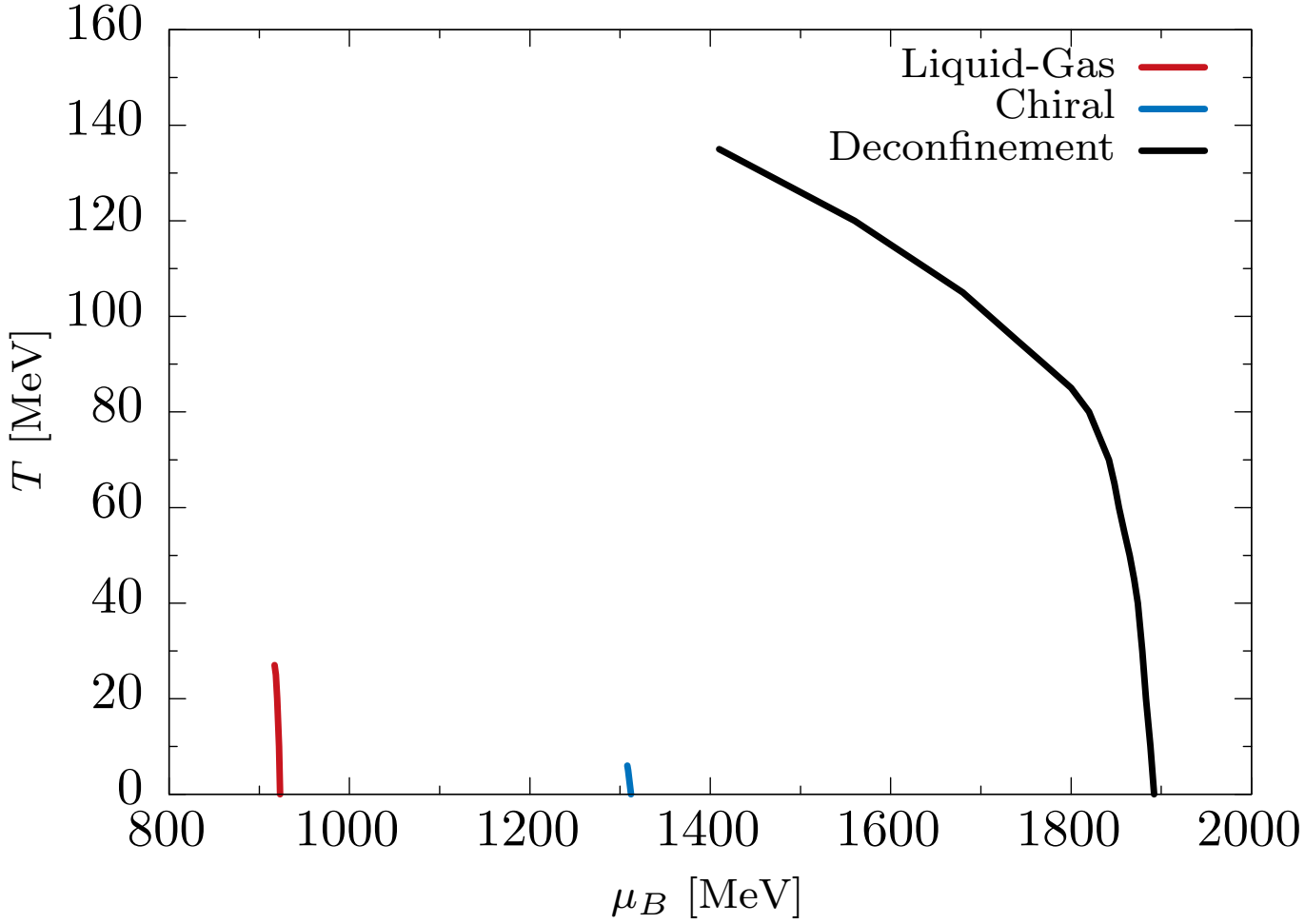

Critical Behavior of χ_2 at $T = 10$ MeV

$$\ln \chi_2 = -\epsilon |\mu_B - \mu_B^c| + r \quad \rightarrow \quad \epsilon \approx 0.67$$

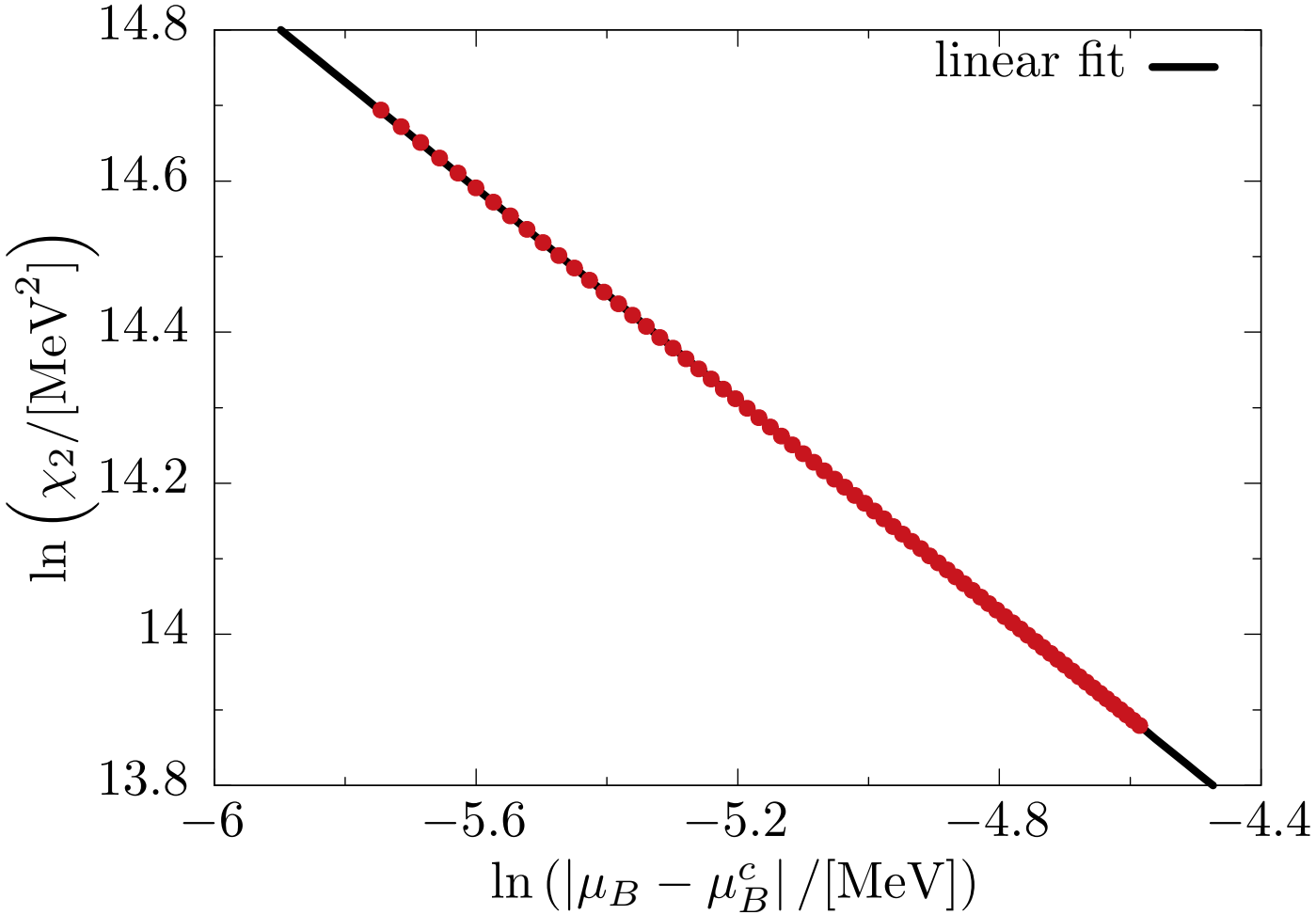

Diagonal contributions to χ_2 ($\alpha b_0 = 390$ MeV)

$$\chi_2 = \sum_{x,y} \chi_2^{xy} = -\sum_{x,y} \frac{\partial^2 \Omega}{\partial x \partial y} \frac{\partial x}{\partial \mu_B} \frac{\partial y}{\partial \mu_B}, \quad x, y = \mu_B, \sigma, \omega, b$$

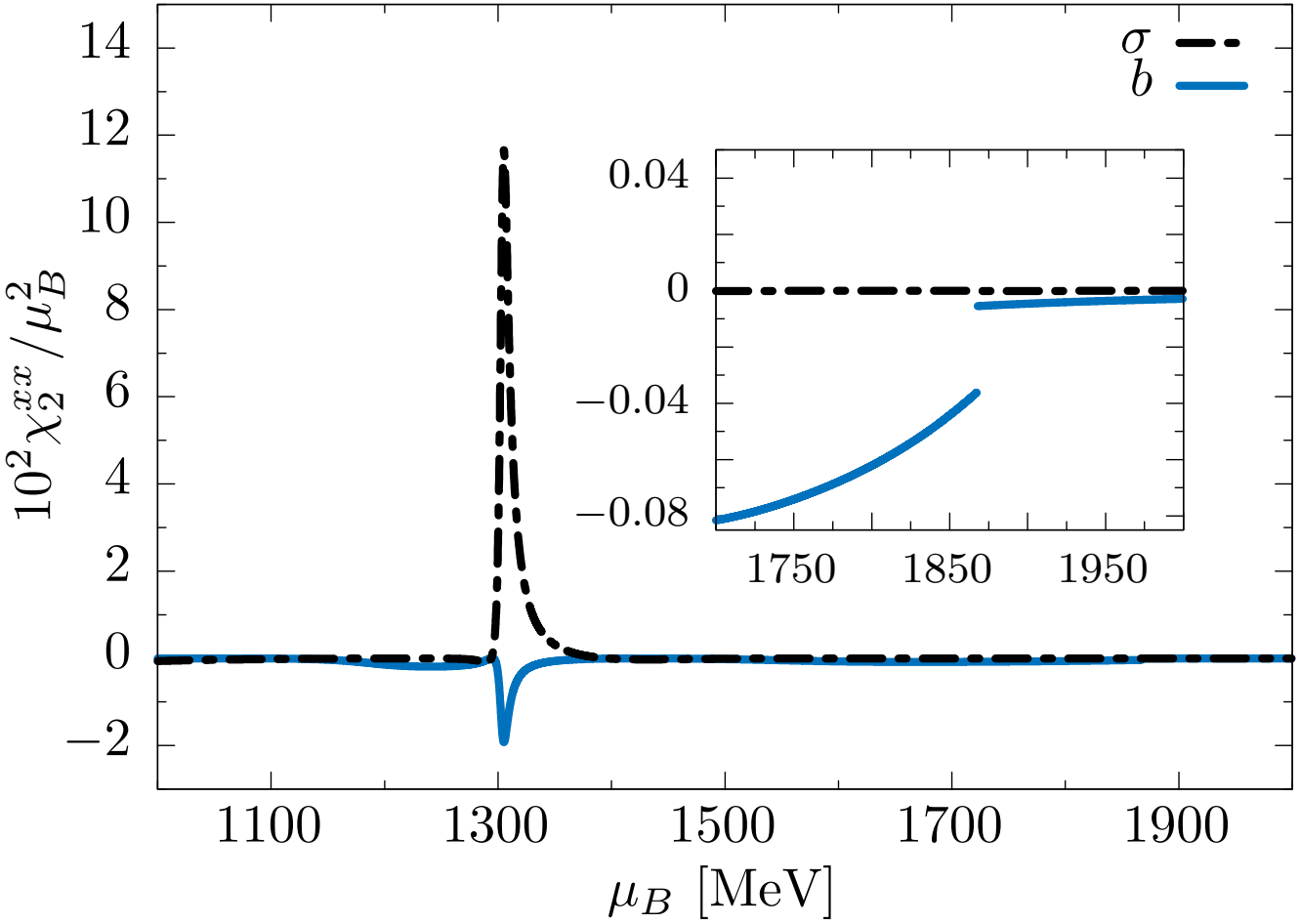

Mean fields at $T = 10$ MeV ($\alpha b_0 = 300$ MeV)

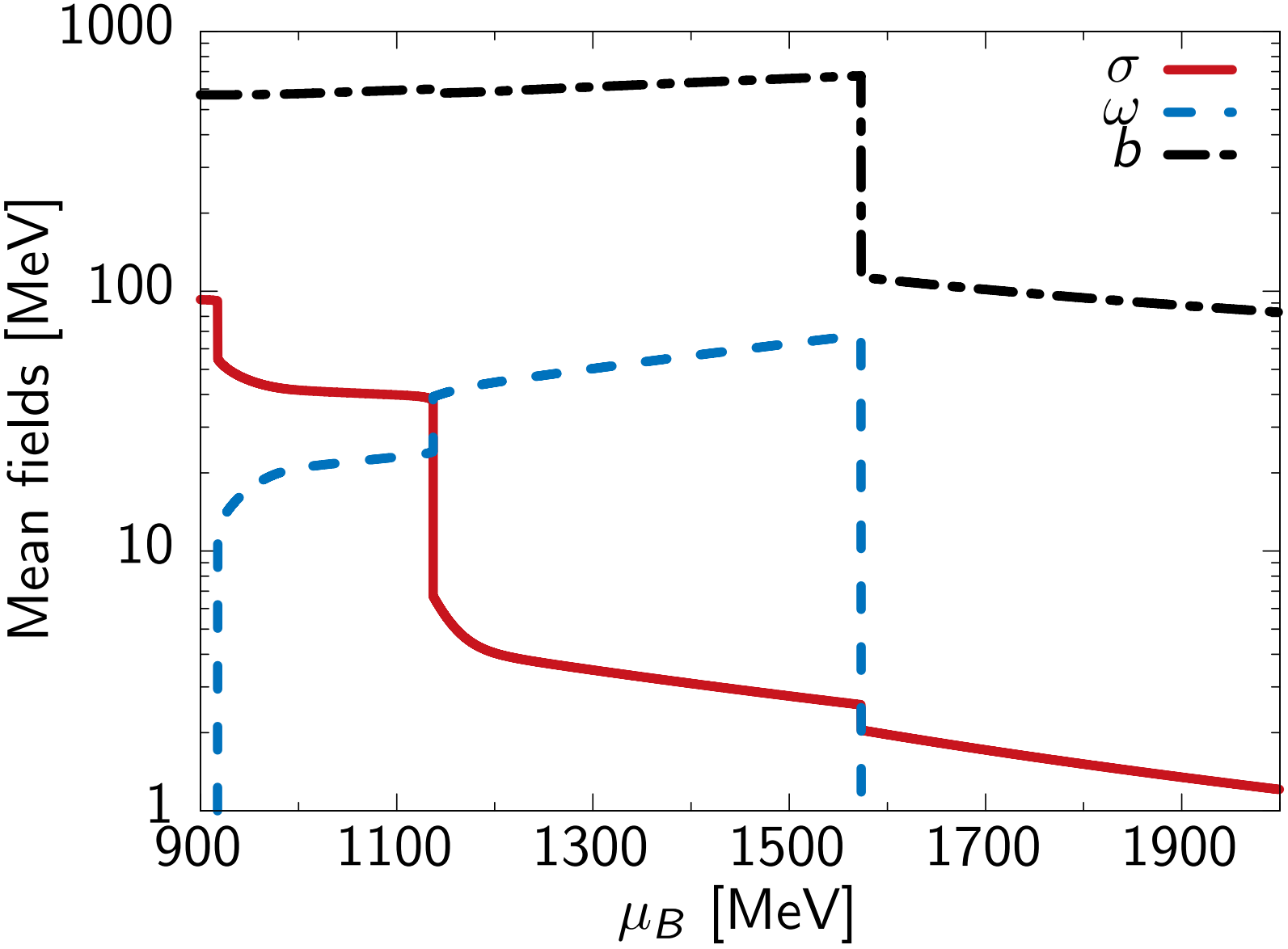

bQM vs PQM Benić *et al*, Phys. Rev. D **91**, 125034 (2015)

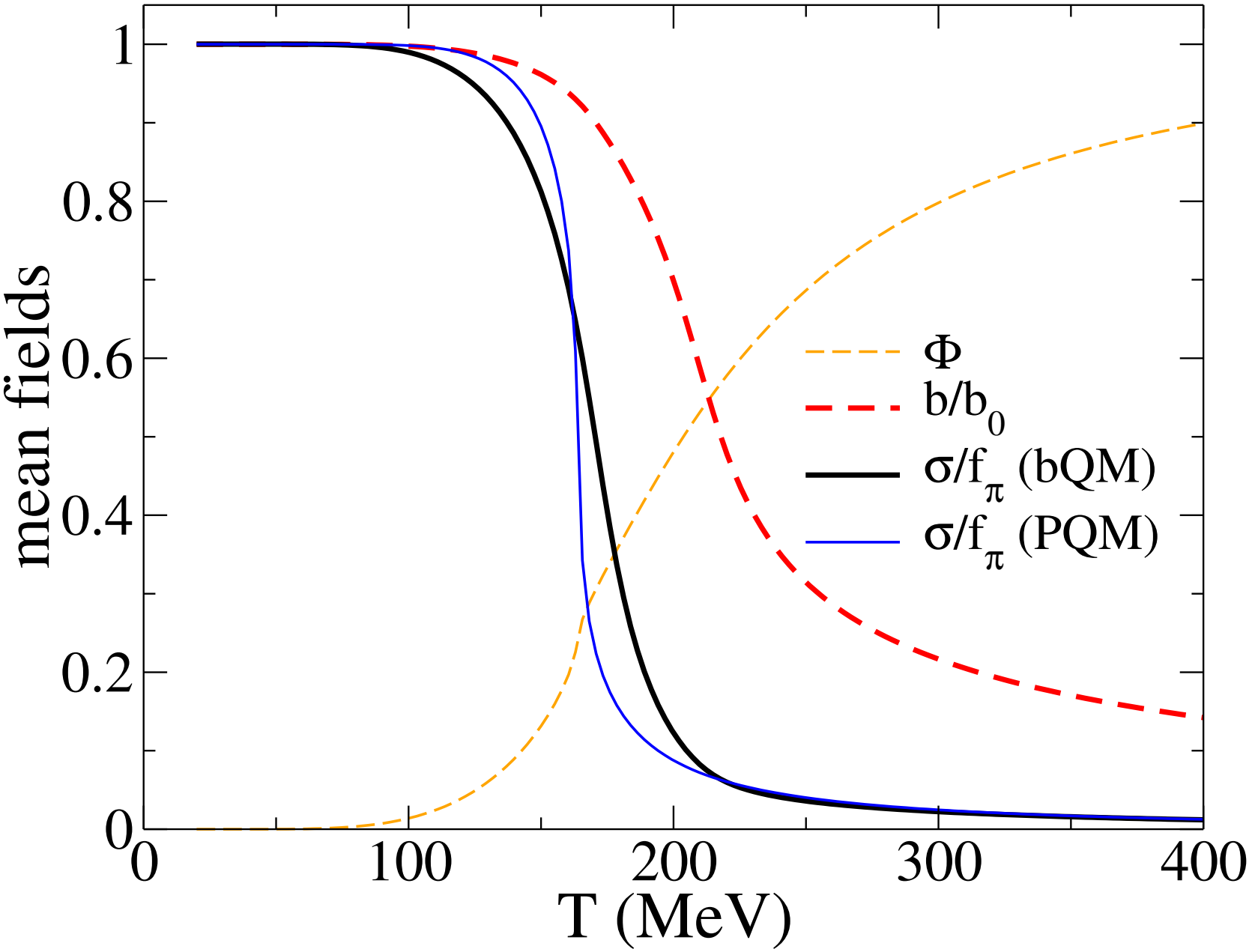

Equation of state at $T = 10$ MeV ($\alpha b_0 = 300$ MeV)

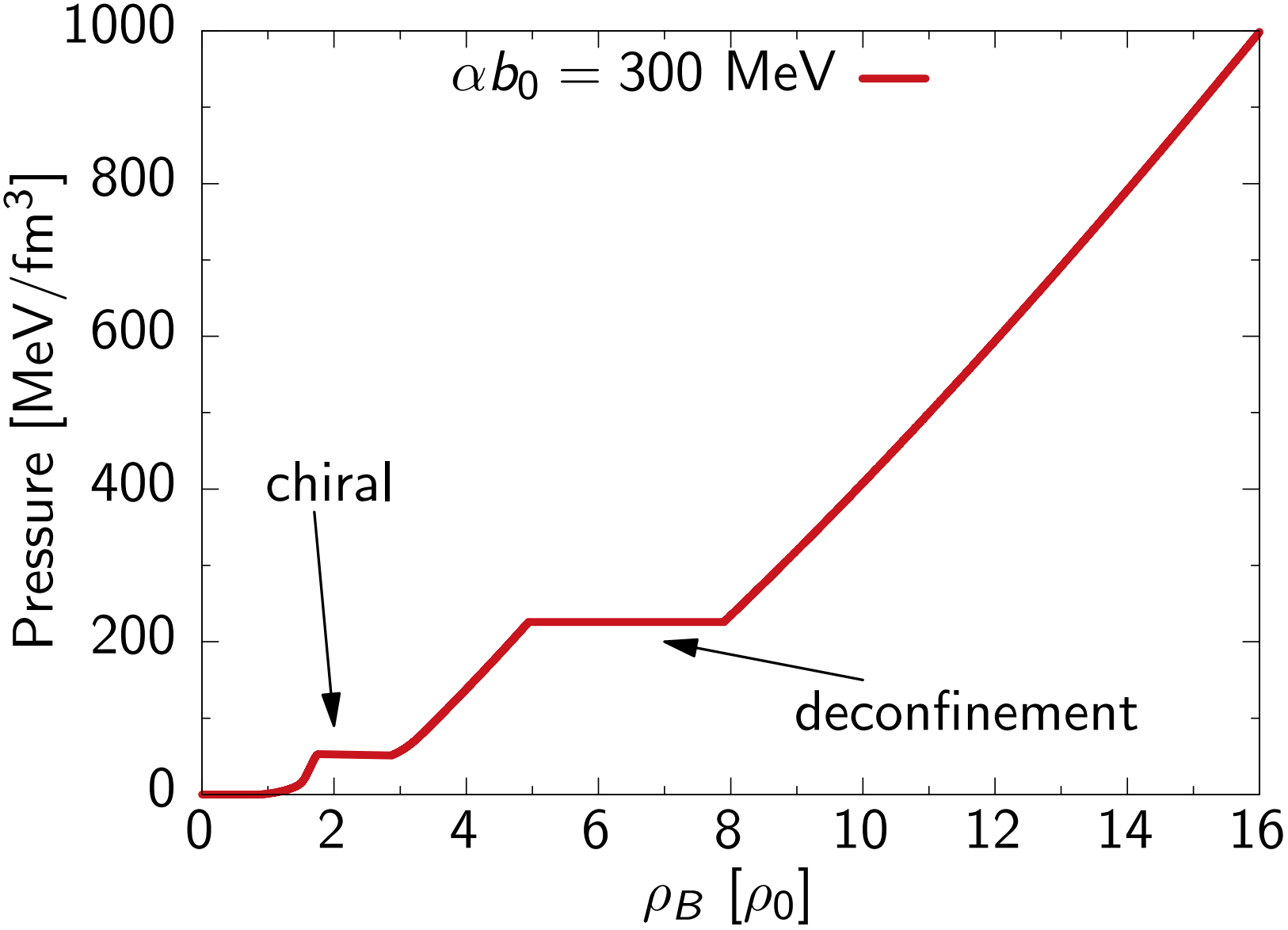

Masses at $T = 10$ MeV ($\alpha b_0 = 300$ MeV)

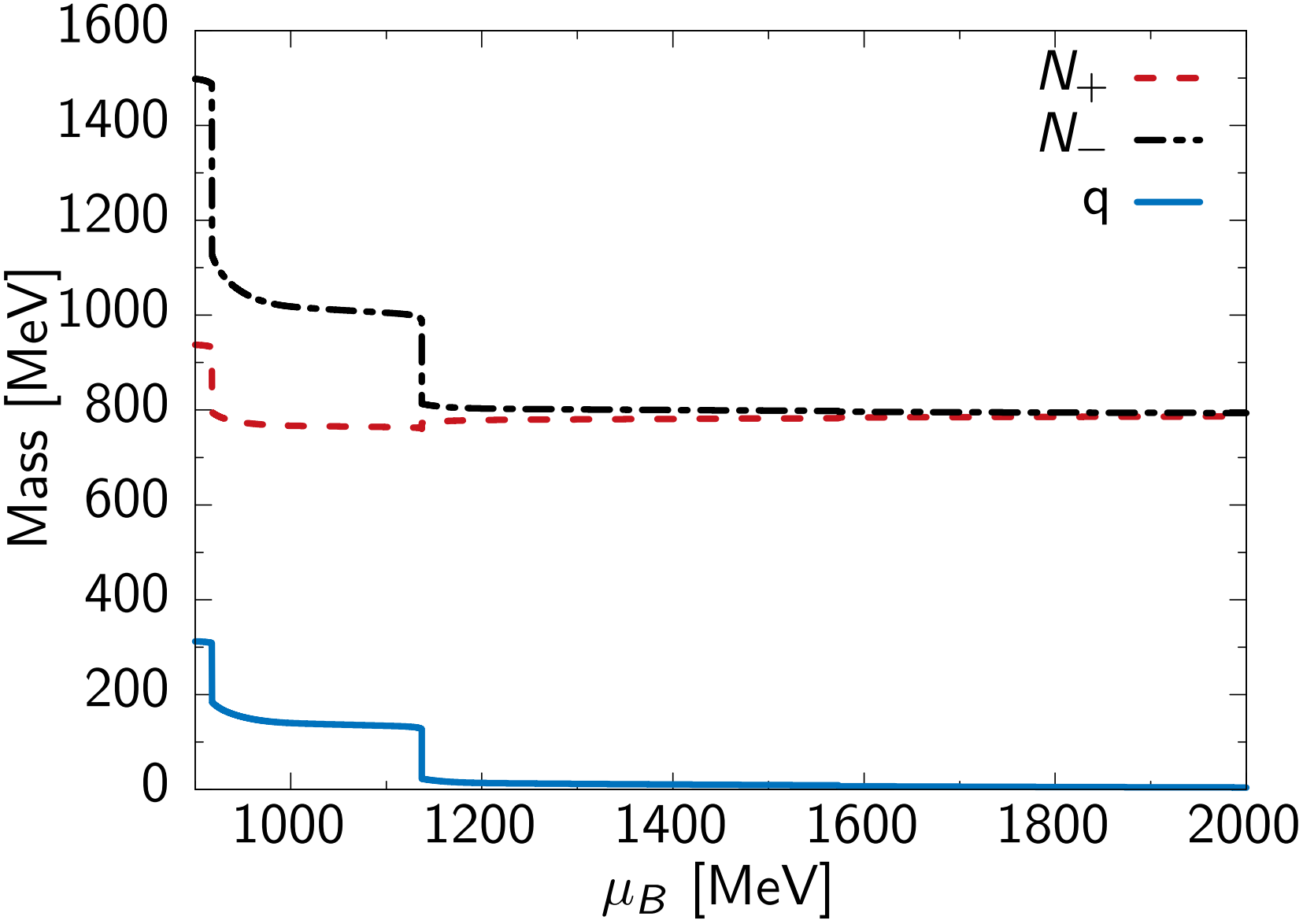

Masses at $T = 10$ MeV ($\alpha b_0 = 390$ MeV)

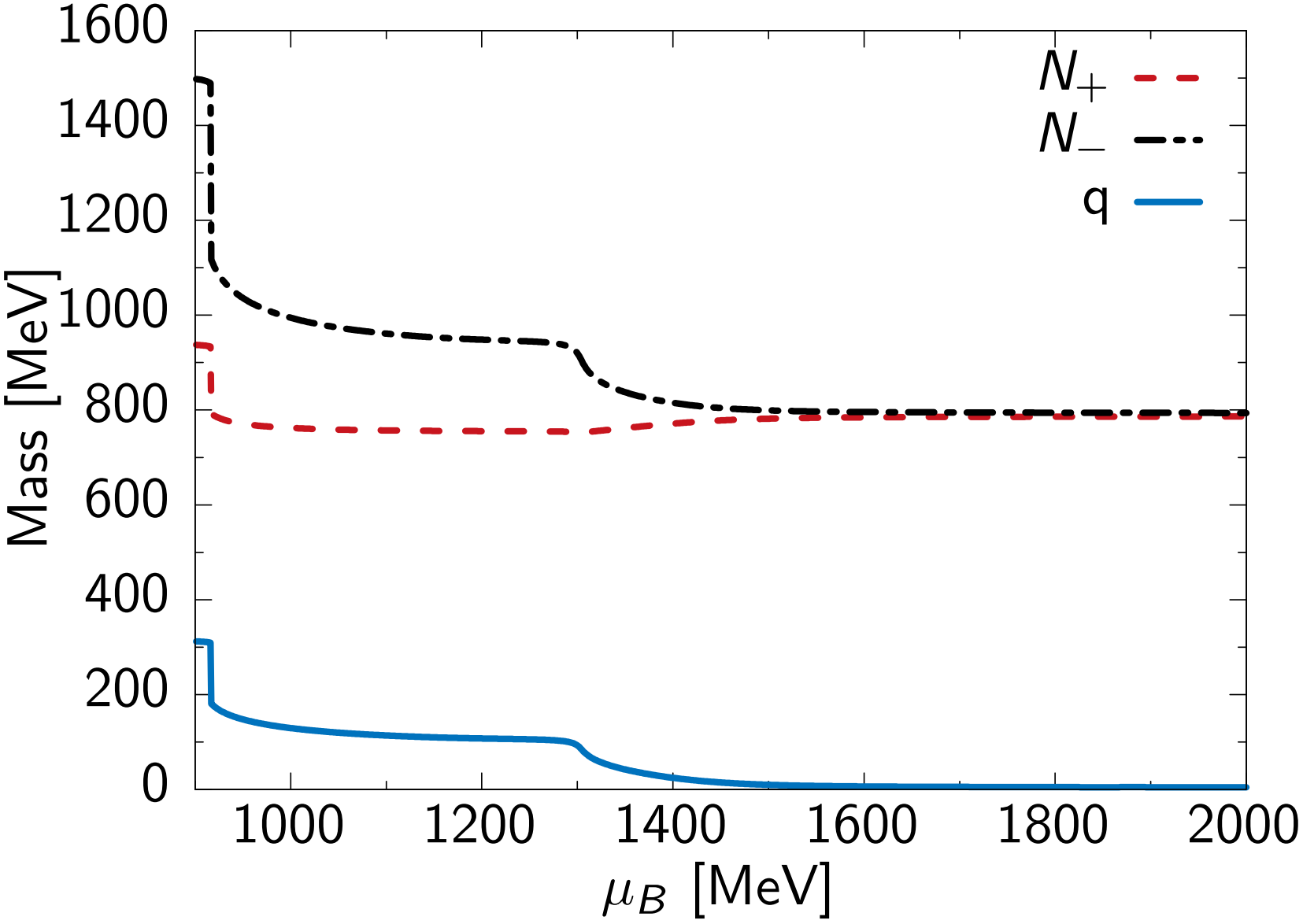

Net-baryon density at $T = 10$ MeV ($\alpha b_0 = 300$ MeV)

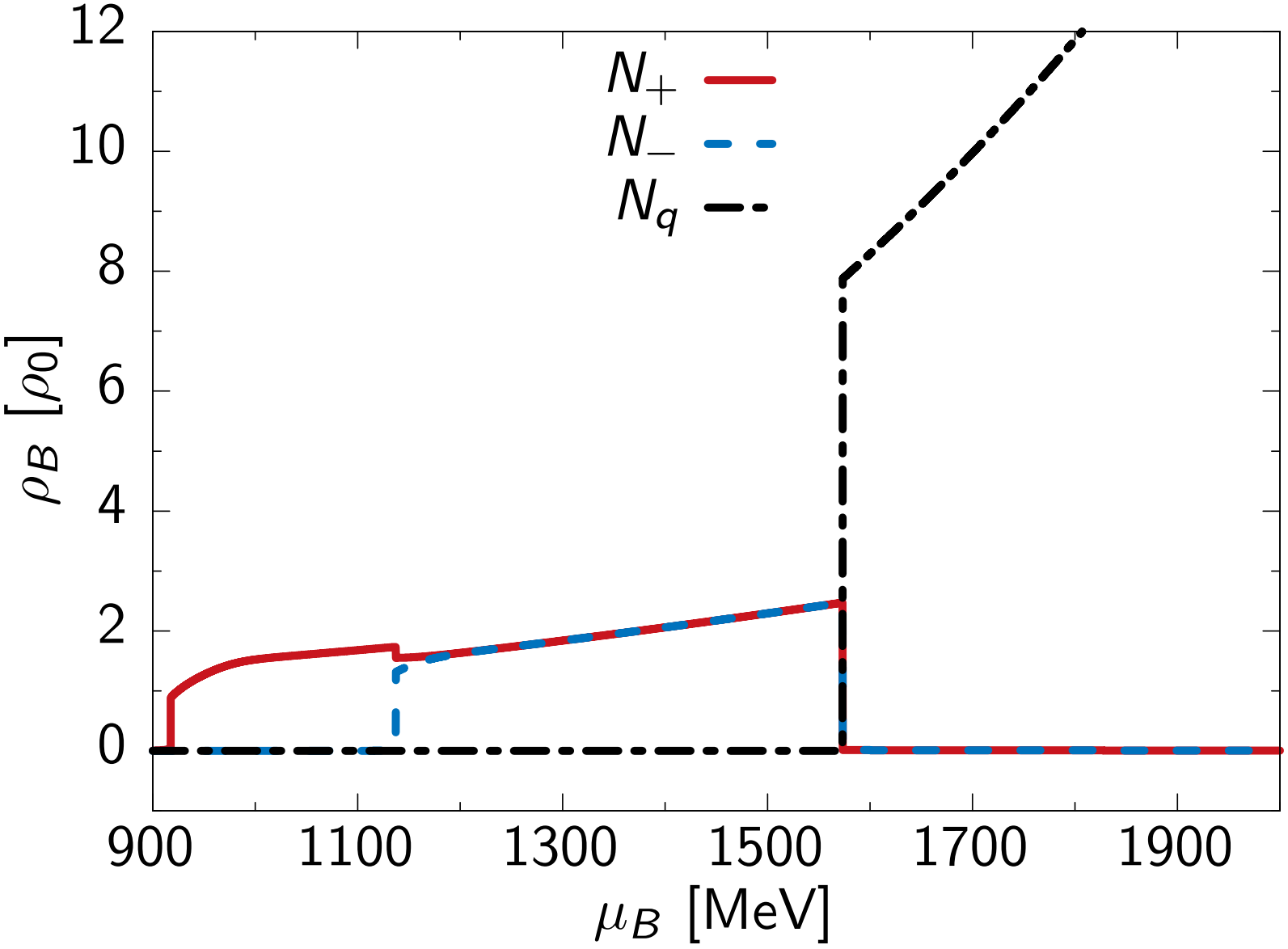

Matter composition at $T = 10$ MeV ($\alpha b_0 = 300$ MeV)

$$Y_x = \frac{\rho_x}{\rho_+ + \rho_- + \rho_q}$$

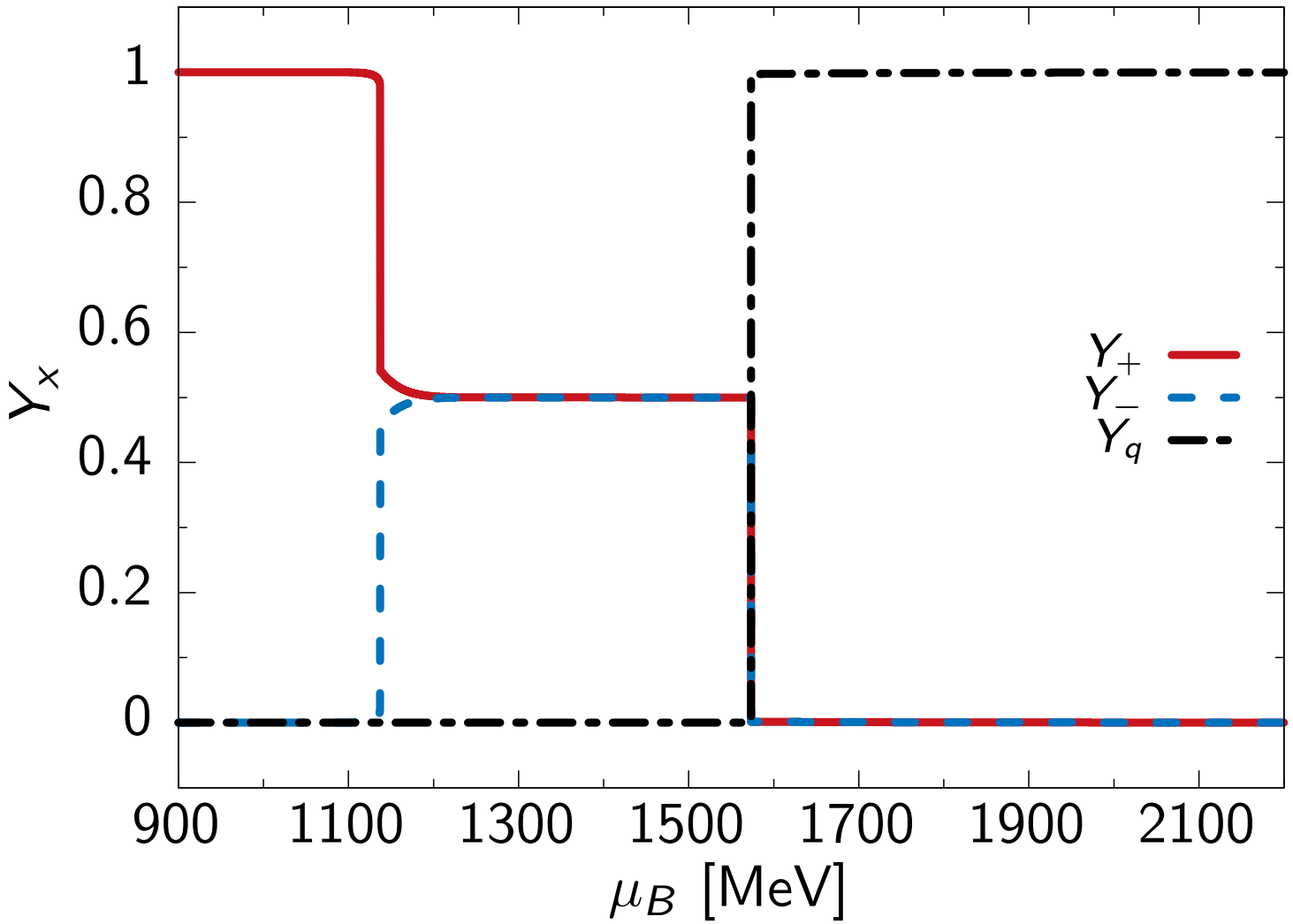

Net-baryon density at $T = 10$ MeV ($\alpha b_0 = 390$ MeV)

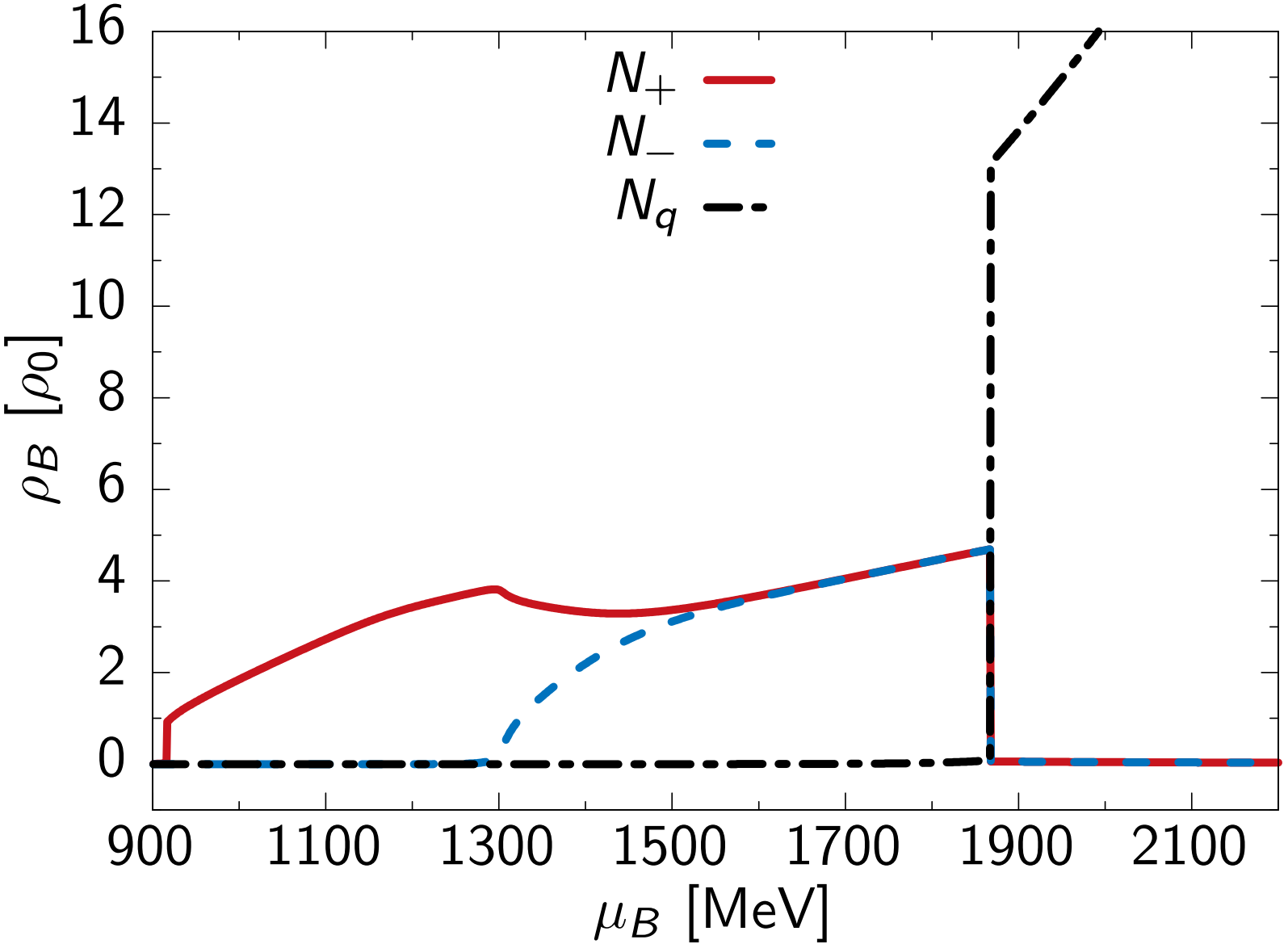

Net-baryon density at $T = 10$ MeV

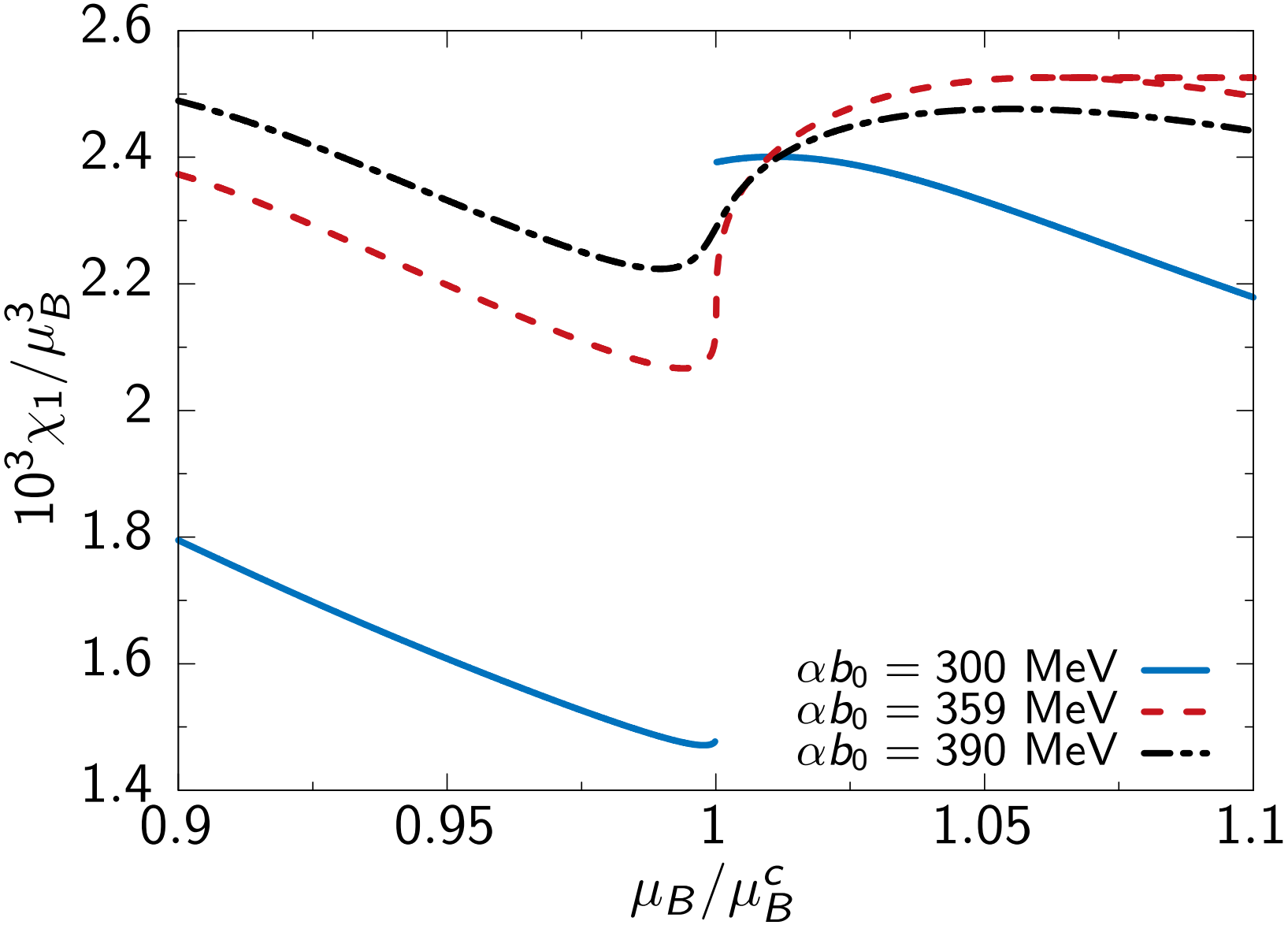

Second-order cumulant at $T = 10$ MeV

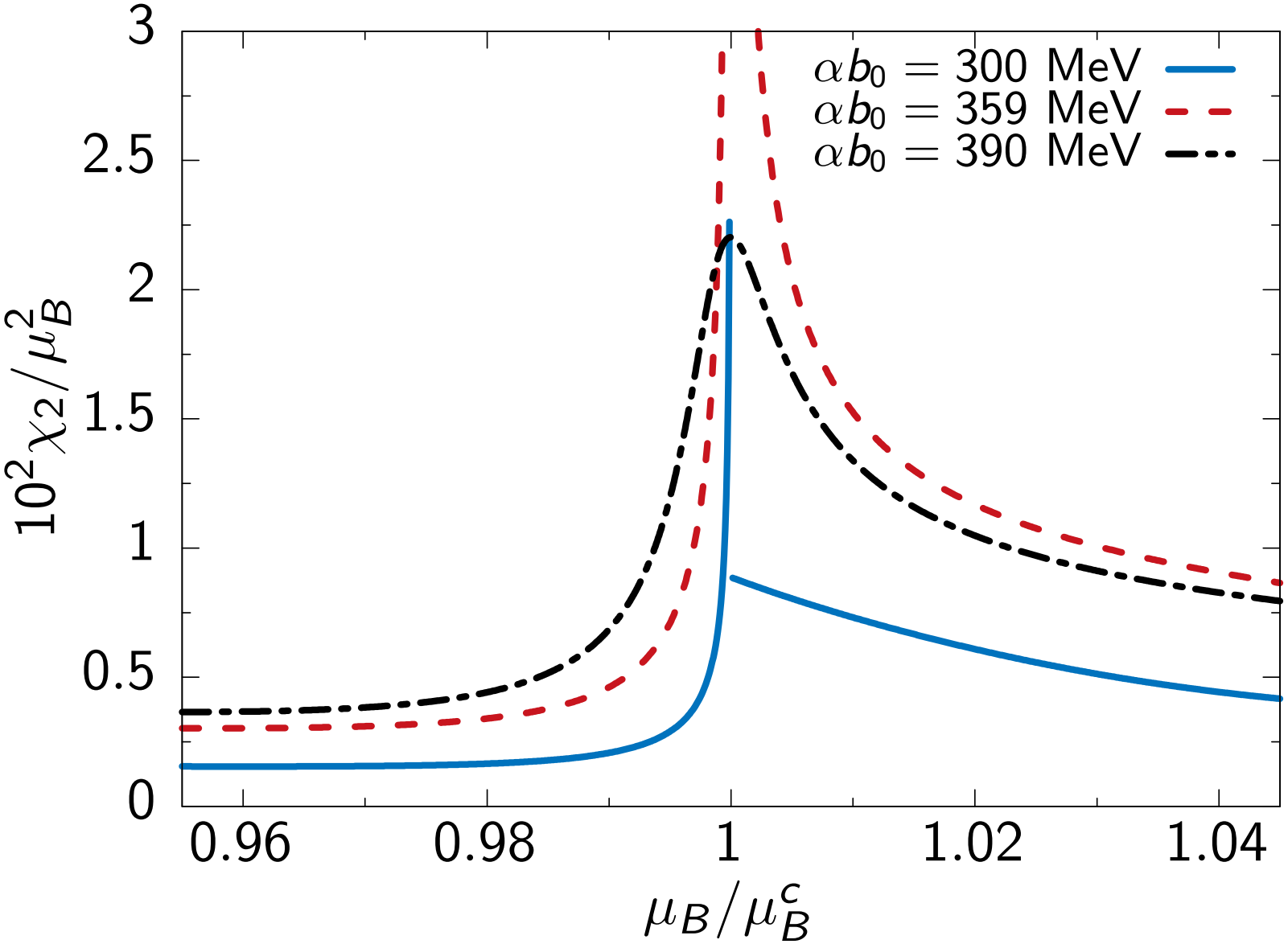

Third-order cumulant at $T = 10$ MeV

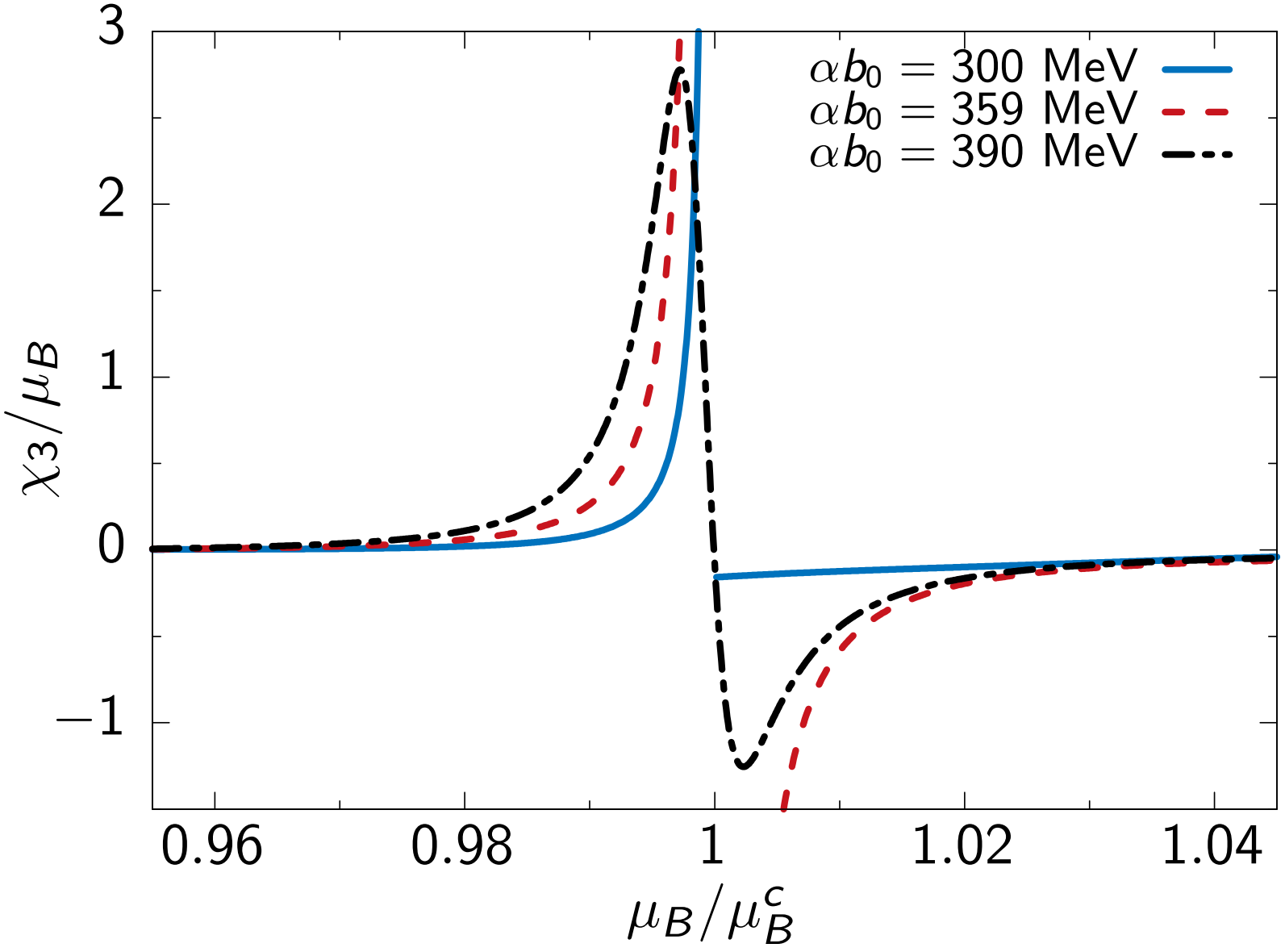

Fourth-order cumulant at $T = 10$ MeV